

Evidence for local structural symmetry-breaking in $\text{Ca}_{1-x}\text{Eu}_x\text{B}_6$

H. Martinho¹, C. Rettori², Z. Fisk³, and S. B. Oseroff⁴

¹*Instituto de Pesquisa e Desenvolvimento, UNIVAP,
12244-050, São José dos Campos, São Paulo, Brazil*

²*Instituto de Física "Gleb Wataghin", UNICAMP, 13083-970, Campinas, São Paulo, Brazil*

³*Department of Physics, University of California, Davis, CA95616 and*

⁴*San Diego State University, San Diego, CA92182*

In this work we present a systematic Raman Scattering study in the $\text{Ca}_{1-x}\text{Eu}_x\text{B}_6$ series ($0.00 \leq x \leq 1.00$). Our results are the first experimental evidence for the occurrence of a local symmetry break of the crystalline structure in this system. The local symmetry of some Boron octahedra is tetragonal instead of cubic. This result may explain the appearance of ferromagnetism in Eu-hexaborades since magnetic ordering is forbidden in the O_h space group of this system.

The hexaborides RB_6 (R = alkaline-earth metal) are one of the most intensively studied groups of intermetallic compounds presenting a large variety of physical ground states.[1] In particular, the family $\text{R}_{1-x}\text{A}_x\text{B}_6$ (A = magnetic rare-earth) has attracted considerable interest due to the intriguing connections between their magnetic,[2] transport,[3] and optical properties.[4, 5] These compounds are cubic with the unit cell belonging to the O_h space group. [6] The divalent alkaline metal occupies the central position on a cube, surrounded by eight B_6 octahedra at each vertex.[6]

In this study we shall focus on the $\text{Ca}_{1-x}\text{Eu}_x\text{B}_6$ series with $0.00 \leq x \leq 1.00$. EuB_6 is a ferromagnetic (FM) metal, characterized by a quite small effective carrier density at high- T ($\sim 10^{-3}$ per unit cell)[7, 8, 9] and presents FM transitions[7] at $T_{C1} = 15.3$ K and $T_{C2} = 12.5$ K. The two transitions exhibit pronounced anisotropy and are sensitive to the application of small magnetic fields.[7] Ferromagnetism is found to arise from the coupling between the half-filled $4f$ shell of Eu^{2+} ions, whose localized electrons account for the measured magnetic moment of $7\mu_B$ per formula unit.[7, 8, 9, 10] The FM transition decreases with Ca content[9, 11] and are completely suppressed for $x \lesssim 0.30$.[12] Electron microscopy data indicates the coexistence of insulating Ca- and metallic Eu-rich regions that percolate at $x \approx 0.30$.[12] Moreover, Urbano *et al* [13] have recently analyzed the behavior of the Eu^{2+} Electron Spin Resonance (ESR) linewidth and reached to the conclusion that the percolation of the impurity bound states starts already at $x \approx 0.15$, i.e., involving next to nearest neighbors.

The intriguing fact is that group theory prevents the occurrence of FM ordering in the O_h space group of RB_6 .[14] The symmetry of the lattice must be lowered to one of its tetragonal or orthorhombic subgroups in order to allow for any FM ordering.[14] High-resolution T -dependent x-ray diffraction measurements by Süllow *et al*[7] failed to observe this symmetry breaking, indicating that its observation must be extremely subtle. However, recent ESR g -value measurements in the $\text{Ca}_{1-x}\text{Eu}_x\text{B}_6$ series have revealed that the symmetry of the crystal may be lower than cubic.[15]

The purpose of our systematic Raman Scattering (RS)

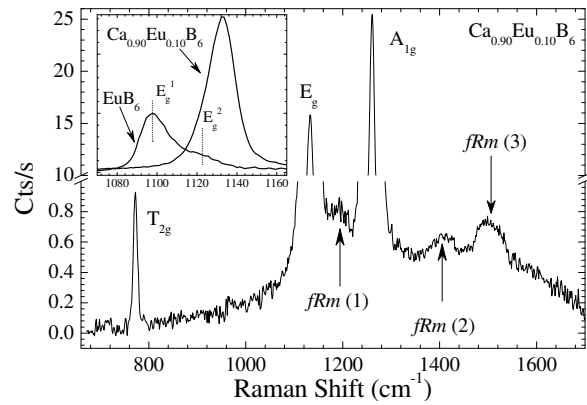


FIG. 1: Room- T unpolarized RS for $\text{Ca}_{0.90}\text{Eu}_{0.10}\text{B}_6$, showing the expected phonons of the O_h cubic structure as well the forbidden ones. The inset shows the doublet structure of the E_g phonon for EuB_6 and the lack of the doubling for $\text{Ca}_{0.90}\text{Eu}_{0.10}\text{B}_6$. This lack also occurs for $\text{Ca}_{0.95}\text{Eu}_{0.05}\text{B}_6$ (not shown).

study in the $\text{Ca}_{1-x}\text{Eu}_x\text{B}_6$ series ($0.00 \leq x \leq 1.00$) is to find an evidence for symmetry-breaking by the crystalline structure that could corroborate the ESR [15] results and justify the appearance of FM ordering in this system. To the best of our knowledge there is no systematic experimental work concerning the T -dependence and polarization selection rules of the RS in hexaborades focusing on the apparent forbidden FM.

For the cubic O_h RB_6 unit cell, the zone-center T_{2g} , E_g , and A_{1g} phonons are Raman-active. These modes correspond to internal displacement of B atoms in the B_6 octahedron.[16] Previous RS works[16, 17, 18, 19, 20, 21, 22, 23] have reported these modes at ~ 780 (T_{2g}), ~ 1150 (E_g), and ~ 1260 (A_{1g}) cm^{-1} . Besides these phonons, additional modes at ~ 200 and ~ 1400 cm^{-1} were also reported. The former was conclusively assigned to two-phonon RS[21] and the latter has no clear assignment yet. We believe that a systematic RS study of the T -dependence and polarization selection rules for these modes may help clarify the enigma concerning the underlying symmetry problem of the RB_6 lattice.

TABLE I: Polarization selection rules in the O_h space group.

configuration	Irreducible Representation
a, b	T_{2g}
a, a	$A_{1g} + E_g + T_{2g}$
a', a'	$A_{1g} + E_g$
a', b'	$A_{1g} + E_g$
c, a	T_{2g}
c, c	$A_{1g} + E_g$
c', c'	$A_{1g} + E_g + T_{2g}$
c', a'	$E_g + T_{2g}$

Single-crystalline samples of $\text{Ca}_{1-x}\text{Eu}_x\text{B}_6$ were grown in a flux of 99.999% pure Al, using the starting elements Eu, Ca, and B with purities of 99.95%, 99.98% and 99.99%, respectively.[6] Magnetic and transport characterization data could be found in ref. [15]. The crystal's shapes were plate-like with typical dimensions of $0.5 \times 4 \times 6 \text{ mm}^3$ (see inset of Fig. 3). The Raman measurements were carried out using a triple spectrometer equipped with a LN₂ CCD detector. The spectra was corrected by the spectrometer response obtained by measuring the emission of a tungsten lamp and comparing it with the emissivity of a black-body at same temperature. The 514.5 nm line of an Ar⁺ ion laser was used as an excitation source. The laser power at the sample was kept below 12 mW on a spot diameter of about 50 μm . The $x = 0.10$ sample was cooled in a cold finger of a He closed-cycle Displex cryostat. All measurements were made in a near-backscattering configuration.

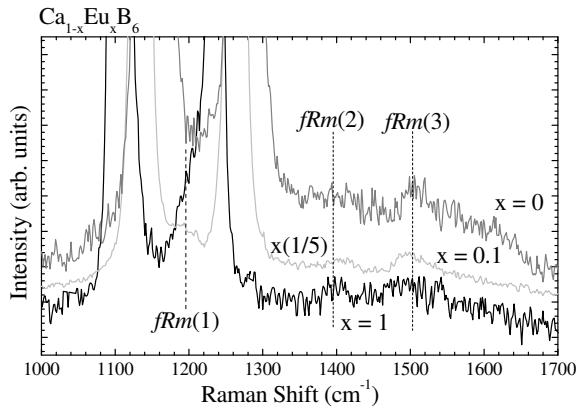
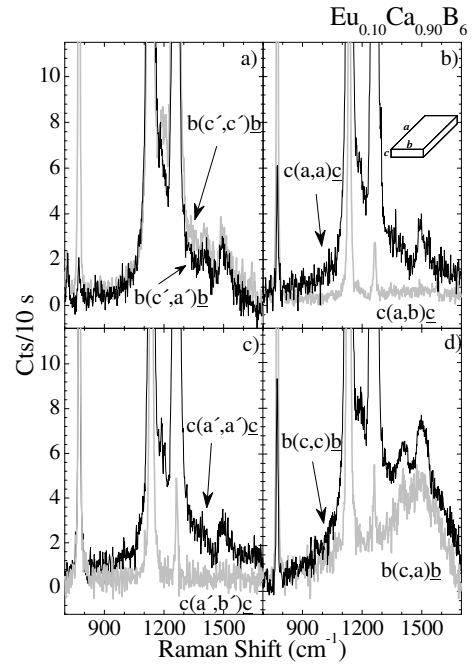
FIG. 2: Room- T unpolarized RS for $x = 0, 0.10$ and 1 , showing the $fRm(1)$ at 1200 cm^{-1} , $fRm(2)$ at 1400 cm^{-1} and $fRm(3)$ at 1500 cm^{-1} .

Fig.1 presents the RS spectrum at 300 K for the $x = 0.10$ sample. This is a representative spectrum of the series and shows the three phonons corresponding to the cubic phase T_{2g} , E_g , and A_{1g} at $775, 1137$ and 1264 cm^{-1} , respectively. Besides these phonons, extra broad modes at $\sim 1170, \sim 1400$ and $\sim 1500 \text{ cm}^{-1}$ are clearly observed. To confirm the phononic origin of these extra modes we used another laser line (488.0 nm) to excite the sample

FIG. 3: Room- T polarized RS spectra for $x = 0.10$ in the configurations listed in table I. The inset of b) shows the typical crystal shape and the a, b and c axes.

and we found that all the modes were observed at the same position with respect to the laser line. The only relevant change was that the spectral intensity response increased by a factor of 5 when the excitation was the 514.5 nm line, indicating a possible resonant behavior. We shall label these extra modes as forbidden Raman modes $fRm(1)$, $fRm(2)$ and $fRm(3)$, respectively. For $x = 0$ the $fRm(1)$ was not observed. Besides, we noticed the presence of a shoulder close to the E_g phonon for $x = 1$ and $x \geq 0.30$. (see inset of Fig.1) This shoulder is always located at $\sim 25 \text{ cm}^{-1}$ above the E_g phonon frequency. For CaB_6 and EuB_6 it was recently attributed to charge unbalancing in the Boron octahedron.[16, 17, 22] It is worth mentioning that for $x = 0.05$ and 0.10 this shoulder is absent, and the E_g peak is symmetric, (see inset of Fig.1).

Fig.2 displays the room- T unpolarized RS for the $x = 0, 0.10$, and 1 samples. The spectra show the $fRm(1)$, (2) and (3) at 1200 cm^{-1} , 1400 and 1500 cm^{-1} , respectively. The $fRms$ are present in all samples, except the $fRm(1)$ that was not observed for $x = 0$. We notice that the peaks are more evident for $x = 0.10$.

In order to get a better insight into the nature of the $fRms$, it is helpful to consider their polarization selection rules. The polarized RS experiments were performed on the ab and ac planes of a monocrystalline sample with $x = 0.10$ at room- T . The a, b and c -axes corresponds to the $[001]$, $[010]$ or $[100]$ crystallographic directions.[6] The smaller crystal thickness determines our c -axis (see inset of Fig.3b)). The data are shown in the Fig.3. The

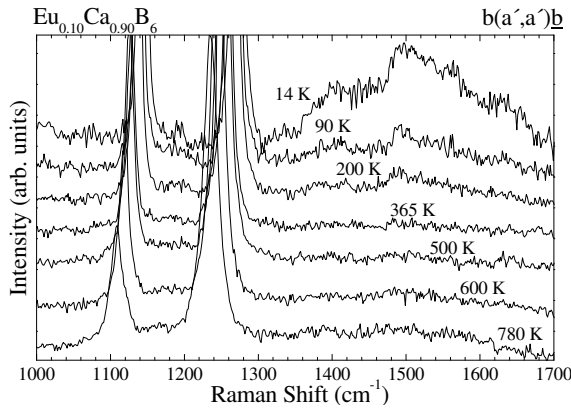


FIG. 4: T -dependence of the RS spectra for the $x = 0.10$ sample at a',a' polarization.

expected selection rules are summarized in Table I. We notice that the phonons A_{1g} , E_g , T_{2g} and $fRm(1)$ follow the expected selection rules for the O_h space group with $fRm(1)$ having the A_{1g} symmetry. However, the $fRm(2)$ and $fRm(3)$ peaks, both having the same symmetry, do not follow the expected selection rules for any cubic configuration presented in Table I. The lack of cubic symmetry is clearly seen when comparing, e.g., the RS signal in a,b and c,a configurations. They must be equal in the O_h space group.

Ogita *et al*[22] observed a broad peak centered at $\sim 1400 \text{ cm}^{-1}$, probably due to the convolution of $fRm(2)$ and $fRm(3)$. These authors assigned it to an overtone of the T_{2g} phonon. We disagree with this interpretation for the following reasons: *i*) the energy of this broad mode is smaller than twice of the T_{2g} phonon frequency; *ii*) the selection rule for this mode is incompatible with any combination of the O_h irreducible representations (IR), contrary to what is expected by the direct product $T_{2g} \otimes T_{2g} = A_{1g} + E_g + T_{1g} + T_{2g}$;^[24] and *iii*) their T -dependence (see below) is incompatible with a two-phonon RS process. Also, these authors observed a low frequency mode at $\sim 200 \text{ cm}^{-1}$, in agreement with previous work.[17, 20, 21] Since this mode was conclusively assigned to two-phonon RS [20] we shall not explore its selection rules.

Another possible origin for the $fRms$ is disorder-activated infrared-activated phonons or combinations between Raman-active and infrared-active modes. Yahia *et al*[18] measured the RS and infrared reflectivity for several hexaborides. Comparing the frequencies of their infrared-active modes with the frequencies of the fRm we conclude that there are no infrared mode, neither possible combinations, that could be assigned to the $fRms$ peaks. Thus, this assumption should be disregarded.

As a different origin for the $fRms$ we may consider the effect of lowering the crystal symmetry. In fact, analyzing the possible symmetry reduction of the cubic O_h group to a tetragonal or orthorhombic ones, we found

that the $fRm(2)$ and $fRm(3)$ have the A symmetry of the tetragonal groups. These results may be understood if one consider that:

- (i) the $fRm(1)$ as a doublet of the A_{1g} phonon originated by the charge unbalancing in the B_6 octahedron, as the E_g doublet, and
- (ii) the $fRm(2)$ and $fRm(3)$ as arising from the local tetragonal symmetry originated by Boron vacancies.

These local symmetry-breaking may allow the FM in this system and justify the difficulties in resolving large scale symmetry changes with bulk techniques as x-ray diffraction. Moreover, our c -axis corresponds to the [001] tetragonal direction which suggests a cooperative character of the distortions, presumably associated to a subtle crystal growth habitus. As we mention above the phonons A_{1g} , E_g , T_{2g} and $fRm(1)$ do not obey the selection rules for the tetragonal symmetry. This suggests that the overall crystal distortion may be very small.

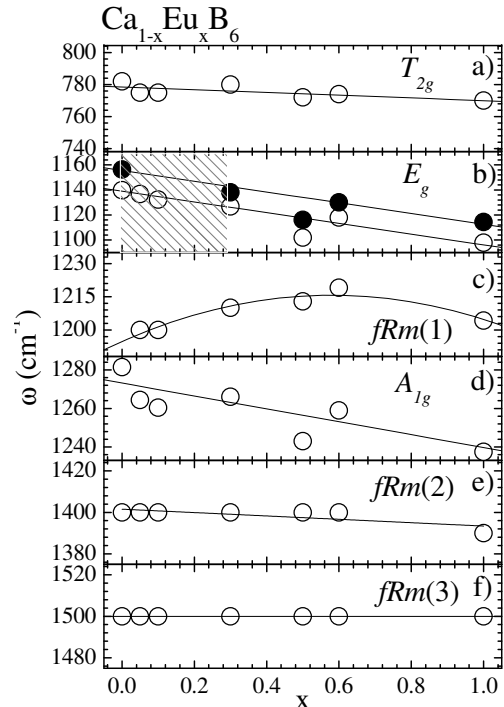


FIG. 5: Room- T phonon frequencies as function of x . Closed circles represents the high energy E_g doublet counterpart and the solid lines are guide for the eyes.

Fig.4 presents the T -dependence of the RS spectra for $x = 0.10$. While the $fRm(1)$ keeps its intensity almost constant, the $fRm(2)$ and $fRm(3)$ present a strong low- T intensity increase. The integrated area of $fRm(2) + fRm(3)$ increases by a factor 6 between 780 and 14 K (not shown). For $T > 400 \text{ K}$, the peak's intensities are nearly constant. We should mention that this T -dependence

is not clearly understood yet. We notice that the T -dependence of the phonon frequencies and linewidths for $x = 0.10$ displayed the expected thermal lattice anharmonicity behavior.[25]

Fig.5 shows the phonon frequencies at 300 K as a function of Eu content x . For the O_h phonons and $fRm(1)$, the frequencies were obtained from fitting the spectra to Lorentzian lineshapes while for the $fRm(2)$ and (3) it was obtained at the position of the maximum intensity. The solid lines are guides for the eyes. The linear softening as function of x for the O_h phonons (Fig.5 a), b) and d)) is consistent with the corresponding increase of the lattice parameter that varies between ~ 4.14 Å for $x = 0$ [22] and ~ 4.18 Å for $x = 1.00$.[7] The lack of E_g doubling can be seen in the $0 < x < 0.30$ interval and it is represented by the dashed area in Fig.5 b). Electron microscopy and resistivity results by Wigger *et al*[12] indicate that in this region there is a phase separation between insulating Ca- and metallic Eu-rich regions that percolate at $x \sim 0.30$. This may reinforce the interpretation about the origin of the E_g doubling that relies in the charge unbalance on the B_6 octahedron. The absence of the E_g doubling in this interval may be related to the lack of long range coherence that screens the doubling of the E_g mode. Increasing the doping beyond $x \sim 0.30$ will reintroduce the long range coherence in the charge distribution enabling again the doubling of the E_g mode. Similar doubling is seen in CaB_6 due to the charge unbalance caused by defects in the sample, which may introduce carriers by doping.[26] Another interesting result is the nearly parabolic behav-

ior of the $fRm(1)$ with a maximum around $x \sim 0.45$. Following our previous idea about the origin of this mode, this behavior may also depend on the competition between insulating-Ca and metallic-Eu-rich regions.

In conclusion, our systematic RS results show the appearance of three $fRms$ in the $Ca_{1-x}Eu_xB_6$ series that does not belong to the expected set of Raman-active phonons of the O_h cubic group. After analyzing different possibilities we suggested that the $fRm(1)$ is a doublet of the A_{1g} phonon, caused by the charge unbalance in the B_6 octahedron, similar to the E_g doublet. Besides, the $fRm(2)$ and $fRm(3)$ peaks arise from the local cubic symmetry-breaking originating from Boron vacancies that induces a local tetragonal environment in the B_6 octahedron. A cooperative behavior of these local tetragonal distortions may explain the appearance of FM in Eu-hexaborates and a tetragonal axis along the smaller crystal dimension. Moreover, their local character would probably justify the difficulties that bulk techniques, such as x-ray diffraction, had in observing this small scale symmetry changes. We should mention that evidences for local distortions of the Boron octahedra were observed in SmB_6 hexaborates by Raman[21] and ESR.[27] It appears that local distortions play an important role in describing the physical properties of hexaborates.

Acknowledgments. This work was supported by the Brazilian Agencies CNPq and FAPESP. We would like to thank Dr. S. Lance Cooper for fruitful discussions and critical reading of the manuscript.

[1] J. Etourneau and P. Hagenmuller, *Philos. Mag. B* **52**, 589 (1985).
[2] J. S. Rhyee *et al* *Phys. Rev. B* **67**, 211407 (2003).
[3] S. Paschem *et al*, *Phys. Rev. B* **61**, 4174 (2000).
[4] G. Caimi *et al*, *Phys. Rev. B* **69**, 12406 (2004).
[5] V. M. Pereira *et al*, *Phys. Rev. Lett.* **93**, 147202 (2004).
[6] Z. Fisk *et al*, *J. Appl. Phys.* **50**, 1911 (1979).
[7] S. Süllow *et al* , *Phys. Rev. B* **57**, 5860 (1998).
[8] L. Degiorgi *et al* , *Phys. Rev. Lett.* **79**, 5134 (1997).
[9] S. Paschen *et al* , *Phys. Rev. B* **61**, 4174 (2000).
[10] W. Henggeler *et al* , *Solid State Commun.* **108**, 929 (1998).
[11] G. A. Wigger *et al* , *Phys. Rev. B* **66**, 212410 (2002).
[12] G. A. Wigger, C. Beeli, E. Felder, H. R. Ott, A. D. Bianchi, and Z. Fisk, *cond-mat/0404570*.
[13] R. R. Urbano *et al*, *cond-mat/0501464*.
[14] W. Opechowski and R. Guccione, in *Magnetism*, ed. G. T. Rado and H. Suhl (Academic Press, New York, 1965), Vol. IIa.
[15] R. R. Urbano, C. Rettori *et al*, private communication (2005).
[16] M. Udagawa *et al* , *J. Phys. Soc. Jpn.* **71**, 314 (2002).
[17] I. Mörke, V. Dvorák, and P. Wachter, *Solid State Commun.* **40**, 331 (1981).
[18] Z. Yahia, S. Turrell, J. -P. Mercurio, and G. Turrell, *J. Raman Spect.* **24**, **207** (1993).
[19] P. Lemmens *et al*, *Physica B* **206&207**, 371 (1995).
[20] P. Nyhus, S. L. Cooper, Z. Fisk, and J. Sarrao, *Phys. Rev. B* **52**, R14 308 (1995).
[21] P. Nyhus, S. L. Cooper, Z. Fisk, and J. Sarrao, *Phys. Rev. B* **55**, 12 488 (1997).
[22] N. Ogita *et al* , *Phys. Rev. B* **68**, 224305 (2003).
[23] P. Teredesai *et al* , *Solid State Commun.* **129**, 791 (2004).
[24] Properties of the Thirty-Two Point Groups, G. F. Koster, J. O. Dimmock, R. G. Wheeler, and H. Statz, MIT Press, Cambridge, Massachusetts (1963).
[25] J. Menéndez and M. Cardona, *Phys. Rev. B* **29**, 2051 (1984).
[26] R. R. Urbano *et al*, *Phys. Rev. B* **65**, 180407 (2002).
[27] H. Sturm, B. Elschner, *Phys. Rev. Lett.* **54**, 1291, (1985).